

## Effects of irradiance on benthic and water column processes in a Gulf of Mexico estuary: Pensacola Bay, Florida, USA

Michael C. Murrell<sup>a,\*</sup>, Jed G. Campbell<sup>a</sup>, James D. Hagy, III<sup>a</sup>, Jane M. Caffrey<sup>b</sup>

<sup>a</sup> US Environmental Protection Agency, Gulf Ecology Division, 1 Sabine Island Dr., Gulf Breeze, FL 32561, USA

<sup>b</sup> Center for Environmental Diagnostics and Bioremediation, University of West Florida, 11000 University Parkway, Pensacola, FL 32514, USA

### ARTICLE INFO

#### Article history:

Received 2 June 2008

Accepted 3 December 2008

Available online 11 December 2008

#### Keywords:

dissolved oxygen

respiration

primary production

nutrient cycles

phytobenthos

net ecosystem metabolism

USA

Florida

Pensacola Bay

### ABSTRACT

We examined the effect of light on water column and benthic fluxes in the Pensacola Bay estuary, a river-dominated system in the northeastern Gulf of Mexico. Measurements were made during the summers of 2003 and 2004 on 16 dates distributed along depth and salinity gradients. Dissolved oxygen fluxes were measured on replicate sediment and water column samples exposed to a gradient of photosynthetically active radiation. Sediment inorganic nutrient ( $\text{NH}_4^+$ ,  $\text{NO}_3^-$ ,  $\text{PO}_4^{3-}$ ) fluxes were measured. The response of dissolved oxygen fluxes to variation in light was fit to a photosynthesis–irradiance model and the parameter estimates were used to calculate daily integrated production in the water column and the benthos. The results suggest that shoal environments supported substantial benthic productivity, averaging  $13.6 \pm 4.7 \text{ mmol O}_2 \text{ m}^{-2} \text{ d}^{-1}$ , whereas channel environments supported low benthic productivity, averaging  $0.5 \pm 0.3 \text{ mmol O}_2 \text{ m}^{-2} \text{ d}^{-1}$  ( $\pm \text{SE}$ ). Estimates of baywide microphytobenthic productivity ranged from  $8.1$  to  $16.5 \text{ mmol O}_2 \text{ m}^{-2} \text{ d}^{-1}$ , comprising about 16–32% of total system productivity. Benthic and water column dark respiration averaged  $15.2 \pm 3.2$  and  $33.6 \pm 3.7 \text{ mmol O}_2 \text{ m}^{-2} \text{ d}^{-1}$ , respectively. Inorganic nutrient fluxes were generally low compared to relevant estuarine literature values, and responded minimally to light exposure. Across all stations, nutrient fluxes from sediments to the water column averaged  $1.11 \pm 0.98 \text{ mmol m}^{-2} \text{ d}^{-1}$  for  $\text{NH}_4^+$ ,  $0.58 \pm 1.08 \text{ mmol m}^{-2} \text{ d}^{-1}$  for  $\text{NO}_3^-$ ,  $0.01 \pm 0.09 \text{ mmol m}^{-2} \text{ d}^{-1}$  for  $\text{PO}_4^{3-}$ . The results of this study illustrate how light reaching the sediments is an important modulator of benthic nutrient and oxygen dynamics in shallow estuarine systems.

Published by Elsevier Ltd.

### 1. Introduction

Estuaries lie at the interface between terrestrial and marine environments, and are sites of intense elemental cycling, particularly of carbon, oxygen, nitrogen, and phosphorus. Human activities have altered estuarine biogeochemistry by increasing nutrient (N, P) loading, thereby increasing organic carbon production and eutrophication (NRC, 2000). When combined with water column density stratification, eutrophication often leads to hypoxic (dissolved oxygen  $< 2 \text{ mg L}^{-1}$ ) or anoxic (dissolved oxygen =  $0 \text{ mg L}^{-1}$ ) bottom waters (Diaz and Rosenberg, 2001).

The numerous estuaries along the Gulf of Mexico coastline have diverse freshwater regimes, ranging from river-dominated to lagoonal systems (Bianchi et al., 1999; Turner, 2001). Most are extremely shallow ( $< 3 \text{ m}$ ) with low tidal energy ( $< 0.5 \text{ m}$  diurnal). River-dominated estuaries such as Pensacola Bay are frequently stratified and are susceptible to hypoxic conditions, but rarely go

completely anoxic (Hagy and Murrell, 2007; Park et al., 2007). Pycnocline depths rarely exceed 2 m, thus sunlight often extends into the bottom layer of the channel regions and to the sediments in the shoal regions. This below-pycnocline production supplies oxygen, thus potentially reducing the incidence of hypoxia. Nevertheless many Gulf of Mexico estuaries experience hypoxia (US EPA, 2001; Bricker et al., 2007; Hagy and Murrell, 2007).

Sediment nutrient fluxes, especially when associated with microphytobenthic activity, can be strongly affected by the ambient light environment (An and Joye, 2001; Eyre and McKee, 2002; Sundbäck et al., 2004). Like many shallow estuaries, Gulf of Mexico estuaries have proportionally large shoal areas that are euphotic, which can support substantial microphytobenthic production (e.g., Schreiber and Pennock, 1995; Stutes et al., 2006). However, most benthic flux studies in Gulf of Mexico systems have ignored the effects of sunlight (Miller-Way et al., 1994; Cowan et al., 1996; Twilley et al., 1999; DiDonato et al., 2006).

This study examined primary production and community respiration in Pensacola Bay, a warm temperate estuary located in the northeast Gulf of Mexico, and focused on summer conditions when the estuary is vulnerable to hypoxia (Hagy and Murrell, 2007). The

\* Corresponding author.

E-mail address: [murrell.michael@epa.gov](mailto:murrell.michael@epa.gov) (M.C. Murrell).

sampling design allowed us to compare metabolic characteristics between channel and shoal environments, and between the upper water column, the lower water column, and the benthos. The study had three objectives. First, we examined the effect of light on benthic oxygen fluxes, which allowed us to derive baywide estimates of benthic microphytobenthic production. Second, we examined the oxygen balance between water column and benthos to arrive at estimates of net ecosystem metabolism. This oxygen balance allowed us to evaluate the conditions that affect hypoxia formation. Third, we examined the role of light in modulating sediment nutrient fluxes.

## 2. Methods

### 2.1. Study area

Pensacola Bay is a river-dominated estuarine system in the northeastern Gulf of Mexico (Fig. 1), of moderate size (370 km<sup>2</sup>), shallow depth (mean 3.4 m) and low tidal energy (Schroeder and Wiseman, 1999; Hagy and Murrell, 2007). The Pensacola Bay watershed is 11,100 km<sup>2</sup>, draining a landscape of pine forests, croplands, pastures and urban development. Escambia and East Bays converge into Pensacola Bay proper, which exchanges with the Gulf of Mexico through a narrow deep pass at the western end of Pensacola Bay and Santa Rosa Sound. Pensacola Bay is moderately productive and strongly influenced by seasonal and episodic freshwater flows (Hagy et al., 2006; Murrell et al., 2007). The system is frequently strongly stratified and becomes hypoxic during summer (Hagy and Murrell, 2007). The hypsography of water depth and light reaching the bottom (Fig. 2) illustrates the high proportion of shoal environments, much of which receives sufficient light to support microphytobenthic production. Approximately half of the bay bottom is euphotic (>10% of surface irradiance), yet seagrasses are sparsely distributed, covering only about 1% (4.6 km<sup>2</sup>) of the bottom (Handley et al., 2007).

### 2.2. Field collection

This study was conducted during summers 2003 and 2004. During 2003, 9 sites were sampled on 9 different occasions located

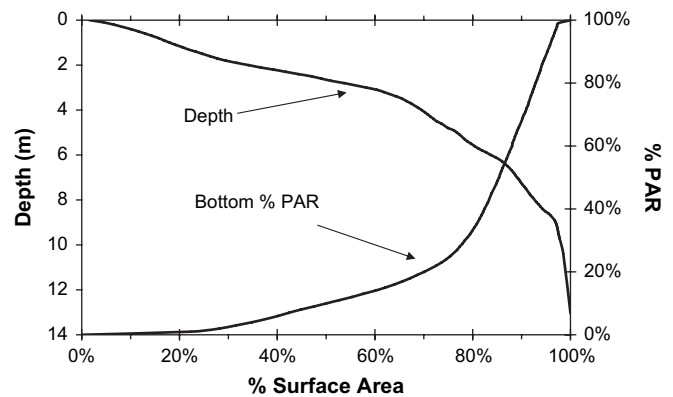


**Fig. 2.** Cumulative distribution of water depth and percentage of PAR reaching the benthos for the Pensacola Bay system. Bathymetry data was digitized from a NOAA navigational chart and projected onto a uniform spatial grid (150 m grid node size). PAR data were collected during 4 summer surveys (1996–1999) at a minimum of 30 sites located throughout Pensacola Bay (US EPA, unpublished data). Attenuation coefficients ( $k$ ) were calculated for each site (either from PAR profiles or as  $1.4/\text{Secchi}$ ) and projected onto the same spatial grid. The percent PAR reaching the bottom was calculated at each grid node as  $\exp(-kz)$ , where  $z$  is depth. Spatial projections (i.e. interpolations) and grid math were performed with an inverse distance algorithm using Surfer® software.

throughout Pensacola Bay. During 2004, 2 sites were sampled repeatedly in lower Escambia Bay, aimed at contrasting shoal and channel oxygen metabolism and nutrient fluxes (Fig. 1). The demarcation between channel (C) and shoal (S) sites was set at 3 m depth, and stations were named accordingly (shoal stations: S1, S2, ..., S7; channel stations: C1, C2, ..., C9). At each station, water column profiles of temperature, salinity, and dissolved oxygen (DO) were measured at 0.25 m depth intervals with a YSI Model 600XL. Secchi disk depth was measured at each site and used to calculate light extinction coefficients ( $k_d$ ) based on an empirical relationship with  $k_d$  derived from underwater photosynthetically active radiation (PAR) measurements. Surface and bottom water was collected by a submersible pump into acid-cleaned polyethylene carboys. For sediments, 12 acrylic cores (10 cm ID  $\times$  40 cm height) were collected by SCUBA, being careful not to disturb the fragile

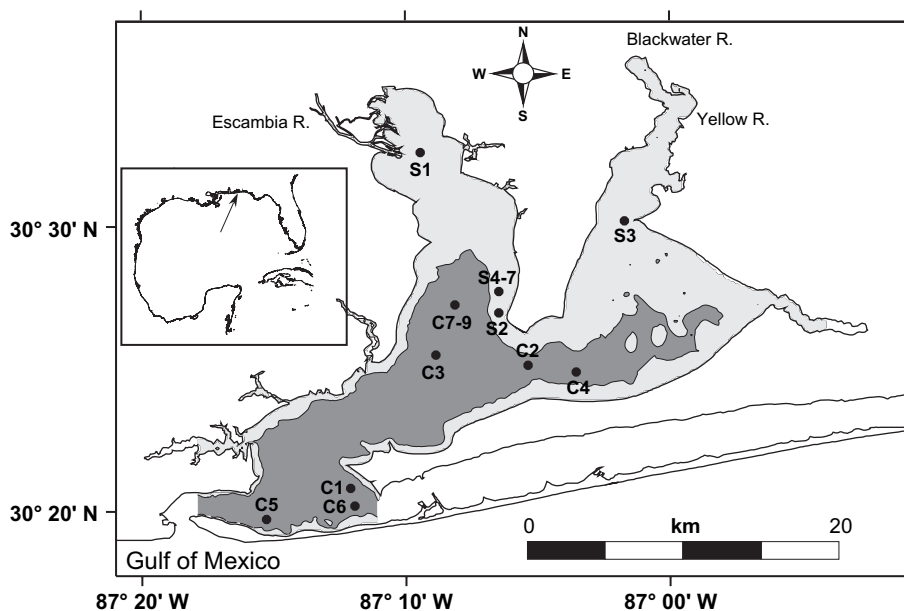


**Fig. 1.** Map of Pensacola Bay system showing its location in the Gulf of Mexico (inset) and sampling locations within the Bay. The shading delineates the 3 m depth contour showing the approximate distribution of well mixed shoal (light shading) and stratified channel (dark shading) environments.

flocculent layer. Additionally, several small sediment cores (2.5 cm) were collected for analysis of sediment characteristics (chlorophyll, % water, % sand, % loss on ignition). Water and sediment samples were placed in dark insulated coolers and immediately returned to the lab for sample processing and flux measurements. At station S2, only upper water column samples were collected. At station C5, sediment samples were not collected.

For water column chlorophyll-*a* (Chl-*a*), samples were filtered onto GF/F filters and frozen at  $-80^{\circ}\text{C}$  until analysis. Chl-*a* was extracted using buffered methanol and measured fluorometrically (Welschmeyer, 1994). For dissolved inorganic nutrients, samples were filtered through a GF/F filter and frozen at  $-80^{\circ}\text{C}$  until analysis. Nutrients ( $\text{NO}_2^- + \text{NO}_3^-$ ,  $\text{NH}_4^+$ ,  $\text{PO}_4^{3-}$ ) were analyzed via standard colorimetric methods (APHA, 1989). For convenience,  $\text{NO}_3^-$  refers to  $\text{NO}_2^- + \text{NO}_3^-$ , DIN (dissolved inorganic nitrogen) refers to  $\text{NO}_3^- + \text{NH}_4^+$ , and DIP (dissolved inorganic phosphorus) refers to  $\text{PO}_4^{3-}$ .

For sediments, the top 1 cm was collected and frozen until analysis. Bulk density, % water, and % loss on ignition (% LOI) were measured by placing homogenized sub-samples (10–20 g) into tared aluminum tins and sequentially measuring wet weight, then dry weight after drying at  $60^{\circ}\text{C}$  for 24 h, and then combusted weight after heating to  $500^{\circ}\text{C}$  for 1 h. Sediment granulometry (% sand, % silt, % clay) was measured following Folk (1974), although only % sand is reported. Sediment Chl-*a* was measured on samples of homogenized sediments, extracted with sonication, centrifuged, and measured fluorometrically, as above. Sediment Chl-*a* was normalized using bulk density and depth of sample and expressed as  $\text{mg Chl-}a\text{ m}^{-2}$ .

### 2.3. Sediment oxygen and nutrient fluxes

Upon returning to the lab, the overlying water was siphoned from the cores and replaced with bottom water collected from the site, being careful to minimally disturb the flocculent surficial sediments. The overlying water completely filled the cores such that there was zero headspace. The core tops were fitted with an o-ring seal, a magnetic stir bar, and a sampling port matching the bevel of the DO probe.

Sediment DO flux measurements were conducted in a 500 L, lighted, temperature-controlled aquarium system. Temperature was set to match bottom water conditions and controlled to  $\pm 1^{\circ}\text{C}$  using an Aquanetics® heat pump through which water was vigorously circulated ( $80\text{ L min}^{-1}$ ). The aquarium was illuminated from each side with a series of eight 165 W cool white fluorescent tubes situated approximately 20 cm from the center of the aquarium, delivering a maximum PAR of  $750\text{ }\mu\text{E m}^{-2}\text{ s}^{-1}$  as measured with a Biospherical® QSL-100 4-pi quantum sensor.

The cores were randomly assigned to 1 of 4 light exposure treatments and randomly positioned in the aquarium with 3 replicates per treatment. Light exposures were varied using 0, 1, 2, layers of neutral density screening (i.e. ordinary fiberglass window screen), which created nominal light exposures averaging 650 (no screening), 370, and  $204\text{ }\mu\text{E m}^{-2}\text{ s}^{-1}$ , respectively. This range in light levels spanned ambient light levels at the sediment–water interface. To avoid exposing sub-surface sediments to light, each core was wrapped with aluminum foil at the sediment–water interface. Heavy black plastic sheeting was wrapped around cores for the dark treatments. As there was some variation among replicate light treatments (CV  $\sim 15\%$ ), light readings were recorded for each individual core. Magnetic stir bars mounted near the top of each core were gently rotated using magnetic stir plates to minimize gradients in DO concentration in the overlying water.

After equilibrating for 1 h, DO concentrations were measured in each core at hourly intervals for 4 h with an Orion 862A DO meter.

The DO meter was calibrated using water-saturated air. Sensor drift was monitored throughout the incubations, however sensor stability was excellent, requiring no drift correction. Water samples (15 or 30 ml) were removed at each time point, filtered and frozen immediately. The volume removed was simultaneously replaced with bottom water collected from the site. The total volume removed and replaced during the incubation was 5–10% of the total overlying water. After incubations were complete, core-specific observations were recorded, including PAR levels, height of the overlying water, obvious signs of benthic activity and overall core quality. DO flux was calculated as the slope of the DO concentration vs. time relationship, normalized by overlying water height, in units of  $\text{mmol O}_2\text{ m}^{-2}\text{ h}^{-1}$ .

### 2.4. Water column DO fluxes

For planktonic DO fluxes, water from each water column layer (upper and lower) was distributed into 18 acid-cleaned 300 ml BOD bottles. Bottle treatments included a dark (6 replicates) plus 4 light treatments (3 replicates each). We opted for additional replication in the dark treatment to improve precision of the respiration measurement. The light treatments used 0, 1, 2 and 3 layers of neutral density screening, except for several early experiments that used 1, 2, 3, and 4 layers of screening. After filling the bottles, DO was measured and recorded for each bottle using an Orion 862A DO meter, as described above. The bottles were placed in racks and situated in the incubator such that bottles and cores were not shading each other. After 24 h of continuous irradiance, the bottles were removed and a second DO measurement was taken from each bottle. Net DO flux was calculated as the change in DO concentration during the incubation period.

Unlike the cores, it was impractical to measure PAR in each BOD bottle for each experiment. Instead, light levels were measured 3 times during the study using a BOD bottle modified with an enlarged opening to allow insertion of the light sensor. The PAR level for 0, 1, 2, 3, and 4 layers of screening averaged 342, 197, 109, 60, and  $39\text{ }\mu\text{E m}^{-2}\text{ s}^{-1}$ , respectively.

### 2.5. P-I parameterization and integration

For sediment and water column incubations, the response of DO flux to varying light exposure was modeled using a standard photosynthesis–irradiance formula,  $P_I = P_m[1 - \exp(-\alpha I/P_m)] + R$ , where  $P_I$  is gross production at light  $I$ ,  $P_m$  is gross production at saturating light,  $\alpha$  is the response of gross production to sub-saturating light, and  $R$  is dark respiration. The parameters  $P_m$  and  $\alpha$  were estimated via non-linear regression (SAS NLIN) and used to drive the daily production model, described below. To avoid extrapolating beyond observations,  $P_m$  was alternatively calculated as the average DO flux at the highest light treatment when in situ midday irradiance exceeded laboratory irradiance. This situation applied to upper water column samples and six lower water column samples (S2 through S7 and C6). Also, in the few instances where the non-linear regression could not find a solution,  $\alpha$  was calculated as the slope of the DO flux response curve at the 2 lowest light treatments and  $P_m$  was calculated as the average DO flux in the highest light treatment.

Gross production was calculated using the model approach of Platt et al. (1990), by numerically integrating gross production  $P$  ( $\text{mmol O}_2\text{ m}^{-2}\text{ d}^{-1}$ ) over upper and lower water column layers of height  $H$  (m) as:  $P = \int_0^D \int_0^H P_m[1 - \exp(-\alpha I_{z,t}/P_m)] dz dt$ . The model used an irradiance matrix ( $I_{z,t}$ ) derived from historical PAR data (June–Aug) collected from the laboratory dock with a LiCOR LI-190 2-pi radiometer between 1999 and 2005 (US EPA, unpublished). From this dataset, the median half-hourly irradiance was

calculated, to represent summer-time average light conditions. Daily irradiance was well-described ( $r^2 > 0.99$ ) by the model,  $I_t = I_{\max} \sin(t/2D + P)$ , where  $I_t$  is PAR at time  $t$  (hour),  $I_{\max}$  is daytime maximum PAR ( $1880 \mu\text{E m}^{-2} \text{s}^{-1}$ ),  $D$  is photoperiod (12.1 h), and  $P$  is the phase shift (6.2 h).

The vertical distribution of irradiance ( $I_z$ ) was calculated as  $I_z = I_0 \exp(-k_d z)$ , where  $I_z$  is PAR at depth  $z$ , and  $I_0$  is surface PAR. The light attenuation coefficient ( $k_d$ ) was calculated from Secchi depth measurements collected at each site using the empirical relationship  $k_d = 1.4/(\text{Secchi depth})$ , which was derived from paired measurements of Secchi depth and  $k_d$  calculated from PAR profiles in Pensacola Bay during the past several years ( $r^2 = 0.65$ ,  $n = 423$ , US EPA unpublished).

## 2.6. Gross production, respiration, and net ecosystem metabolism

Vertically integrated rates were computed by layer for gross production, respiration, and net ecosystem metabolism. The boundary between upper and lower layers was defined by the pycnocline or, when stratification was absent, the midpoint of the water column. The pycnocline was identified by visual inspection of sigma- $t$  profiles; in most cases, a clearly defined and rapid change in density was observed. The bottom layer of the water column was assumed to end 18 cm above the sediment surface, the average height of headspace in core incubations. This accounted for this small portion of the lower water column that was included in the measured sediment-flux rates.

Gross production was integrated separately for the two water column layers using layer-specific  $\alpha$  and  $P_m$  parameter estimates at 20 depth steps per layer. If stratification was absent, the results were summed after integration and represented as a single (upper) layer. Benthic gross production was integrated similarly over the day at a single depth step using  $I_z$  calculated at the sediment–water interface. Water column integrated respiration was calculated as the product of the layer-specific volumetric respiration rate and the thickness (m) of the layer. Net ecosystem metabolism (NEM) was calculated as the difference between daily integrated (plankton plus benthos) gross production and respiration. Gross production, community respiration and NEM are reported in oxygen units (e.g.,  $\text{mmol O}_2 \text{m}^{-2} \text{d}^{-1}$ ), but are also scaled to carbon units assuming

$\text{RQ} = \text{PQ} = 1$  to facilitate comparisons with carbon-based literature values.

## 3. Results

### 3.1. Site conditions

Typical of summer in Pensacola Bay, the water column tended to be well-mixed in the shoal regions and intensely stratified in the channel (Table 1). Salinity ranged from near zero at shoal stations adjacent to the Escambia and Yellow river mouths (S1 and S3, respectively) to over 30 in the bottom waters near the Gulf of Mexico (C1, C5, and C6). The channel sites were strongly stratified (except C9); the average difference between surface and bottom salinity was 22. At these sites, the pycnocline was sharply defined, typically at 2–3 m. Water column Chl- $a$  averaged  $6.9 \pm 3.7 \mu\text{g L}^{-1}$  ( $\pm\text{SD}$ ) and was usually higher in the surface (upper) layer. DO tended to be near saturation in the upper layer ( $\sim 7 \text{ mg L}^{-1}$ ), and depleted in the lower layer when stratification was present ( $1\text{--}5 \text{ mg L}^{-1}$ ). Nominal midday benthic PAR averaged  $25 \mu\text{E m}^{-2} \text{s}^{-1}$  and  $330 \mu\text{E m}^{-2} \text{s}^{-1}$  at channel and shoal sites, respectively (Table 1).

Sediments were of 2 distinct types: sandy and silty (Table 2). Sandy sediments (average 95.8% sand) were observed in the shoals while silty sediments (average 8.4% sand) were observed at channel sites. Sandy sites had higher average Chl- $a$  than silty sites (Kruskal–Wallis,  $p = 0.02$ ), whereas silty sites had higher organic content (based on LOI,  $p < 0.01$ ). Water content of silty sediments tended to be higher compared to sandy sediments, but was variable (Table 2).

### 3.2. DO flux parameterization

Thirty of 31 water column experiments and 14 of 15 benthic experiments (Figs. 3 and 4) exhibited a significant positive DO flux response to light exposure (Pearson's  $r$ ,  $p < 0.05$ ), from which the  $P$ – $I$  parameters, ( $\alpha$  and  $P_m$ ), were derived and used to calculate daily integrated production. In the sediments, the DO flux response to light was generally linear, whereas in the water column, DO flux consistently showed saturation at high light. Variability among replicates was higher in sediments than the water column. At many channel sites, sediments showed only a weak DO flux response to irradiance. Sediment DO flux remained negative across the entire

**Table 1**  
Water properties during study. Shoal and channel regions were distinguished at 3 m depth. The pycnocline (Pycno) was determined by visual inspection of water column salinity profiles. The water column attenuation coefficient ( $k$ ) was calculated as  $1.4/\text{Secchi depth}$ . Temperature reported as water column averages, and varied little from surface to bottom ( $< 2^\circ\text{C}$ ). Chlorophyll- $a$  (Chl- $a$ ), salinity and dissolved oxygen (DO) are reported for the upper (UWC) and lower (LWC) water column separately. The lower DO concentrations represent initial concentration measured in incubation experiments and were sometimes higher than in situ bottom concentrations (C7 and C8) due to reaeration. Benthic PAR was calculated from depth and attenuation coefficient assuming midday irradiance of  $1880 \mu\text{E m}^{-2} \text{s}^{-1}$ .

Station	Date	Depth (m)	Pycno (m)	$k$ ( $\text{m}^{-1}$ )	Average Temp ( $^\circ\text{C}$ )	Upper Chl- $a$ ( $\text{mg m}^{-3}$ )	Lower Chl- $a$ ( $\text{mg m}^{-3}$ )	Upper Salinity (psu)	Lower Salinity (psu)	Upper DO ( $\text{mg L}^{-1}$ )	Lower DO ( $\text{mg L}^{-1}$ )	Benthic PAR ( $\mu\text{E m}^{-2} \text{s}^{-1}$ )
S1	30 Jul 03	2.3		2.00	26.3	1.7	0.7	0.1	0.2	5.5	4.8	19
S2	1 Aug 03	1.0		1.56	29.6	9.2	9.2	2.3	2.3	7.4	7.5	397
S3	5 Aug 03	1.7		1.75	28.2	5.2	3.7	0.3	0.3	6.1	6.5	96
S4	2 Jun 04	1.3		1.09	27.0	6.6	9.4	14.9	20.9	7.1	7.5	459
S5	29 Jun 04	1.3		1.17	28.8	13.1	9.4	8.5	10.4	7.4	6.7	413
S6	29 Jul 04	1.3		1.27	30.8	8.5	12.1	10.7	17.0	6.3	6.4	359
S7	9 Sep 04	1.3		0.93	27.7	4.3	5.8	20.9	22.0	6.3	6.2	559
C1	22 Jul 03	3.8	3.1	1.08	28.6	11.8	1.7	11.1	30.3	6.9	2.7	31
C2	25 Jul 03	3.0	2.0	1.56	28.0	9.5	8.6	1.8	13.4	7.5	5.1	18
C3	28 Jul 03	6.0	1.7	1.40	28.9	9.1	2.0	2.4	29.9	7.5	1.3	0
C4	29 Jul 03	4.9	2.9	1.40	29.2	11.2	2.5	2.9	26.2	7.3	1.0	2
C5	6 Aug 03	9.7	2.9	1.00	28.5	8.3	1.7	3.5	33.1	7.3	5.0	0
C6	7 Aug 03	5.6	1.1	1.00	28.2	11.3	2.1	6.4	31.2	7.2	4.3	7
C7	28 Jun 04	3.7	2.4	0.82	29.3	6.2	7.7	10.3	27.1	7.3	4.6	89
C8	27 Jul 04	3.7	2.1	1.27	29.3	9.5	10.9	9.3	27.8	7.4	4.8	17
C9	8 Sep 04	3.7		0.93	27.2	4.4	3.8	21.8	21.8	6.2	5.7	59



**Table 2**

Sediment properties during study. Variables include Chl-*a* (mg m<sup>-2</sup>), % water, % loss on ignition (% LOI) and % Sand. Averages (±SE) by region and predominant sediment type (sandy/silty) are included at the bottom.

Station	Chl- <i>a</i>	% Sand	% Water	%LOI
S1	61.6	4.5	78.2	13.2
S2	417.6	91.2	19.5	0.3
S3	315.9		25.3	0.5
S4	196.8	99.8	21.7	0.5
S5	67.7	100.0	24.2	0.3
S6	234.6	92.2	24.3	0.5
S7	150.7	91.5	23.9	0.3
C1	166.0		23.0	0.6
C2	149.5	100.0	37.4	1.4
C3	91.7	4.6	79.7	14.1
C4	62.4		79.8	13.7
C6	177.8		49.8	2.7
C7	87.8	16.4	16.4	15.1
C8	18.0	9.2	9.2	17.7
C9	14.6	7.2	7.2	10.0
Shoal Sites	206.4 ± 49.0	79.9 ± 15.2	31.0 ± 7.9	2.2 ± 1.8
Channel Sites	96.0 ± 22.5	27.5 ± 18.2	37.8 ± 10.4	9.4 ± 2.4
Sandy Sites	202.8 ± 48.7	95.8 ± 1.9	25.2 ± 2.6	0.54 ± 0.17
Silty Sites	54.7 ± 16.5	8.4 ± 2.2	38.1 ± 16.7	14.0 ± 1.3

experimental light gradient at two channel sites (C8 and C9) and one shoal site (S1). Water column (upper and lower) DO fluxes were strongly light-dependent, but the response of the 2 water column layers was inconsistent. In some instances, the DO flux response to light was greater in the upper water column than in the lower water column (S2, C1, C3, C4, C5, and C6), but the reverse pattern was also observed (S4, S7, C2, C7, C8). These differences in water column response were largely attributable to differences in Chl-*a* in the 2 layers (Table 1).

Table 3 summarizes the biomass-normalized photosynthetic parameters ( $\alpha^B$  and  $P_m^B$ ) for the 2 water column layers and the benthos. For the water column,  $\alpha^B$  was similar at all locations, ranging from 2.99 to 3.24  $\mu\text{mol O}_2(\text{mg Chl-}a \text{ h})^{-1} [\mu\text{E m}^{-2} \text{ s}^{-1}]^{-1}$ . The differences among site location (channel vs. shoal) and water column layer (upper vs. lower) were not significant (ANOVA,  $p > 0.3$ ). In the benthos,  $\alpha^B$  averaged 0.038  $\mu\text{mol O}_2(\text{mg Chl-}a \text{ h})^{-1} [\mu\text{E m}^{-2} \text{ s}^{-1}]^{-1}$  with values similar at channel and shoal sites, but about 2 orders of magnitude lower than the water column averages. Water column  $P_m^B$  varied 4-fold, from 285 to 1173  $\mu\text{mol O}_2[\text{mg Chl-}a]^{-1}$  and was higher at the channel sites compared to the shoal sites (ANOVA,  $p = 0.01$ ). Benthic  $P_m^B$  averaged 29  $\mu\text{mol O}_2[\text{mg Chl-}a]^{-1}$  and was about 3-fold higher at the shoal sites compared to the channel sites, though not statistically significant. Benthic  $P_m^B$  was about 1 order of magnitude lower than the water column values.

### 3.3. Gross production, respiration and net ecosystem metabolism

Daily integrated gross production differed by site and water column layer (Table 4). Channel sites had higher gross production than shoal sites (ANOVA,  $p < 0.01$ ). When the water column was stratified, 78 ± 22% (±SD) of the gross productivity occurred in the upper water column (excluding C9). Lower layer gross production was highest at stations C6, C7, and C8 where the pycnocline was shallow (Table 1). Very low production occurred at site S1, which was located in turbid waters near the mouth of the Escambia River. At shoal sites, benthic production accounted for an average of 28% of integrated production, whereas at channel sites benthic production averaged only 0.7% of integrated production. Benthic production was positively related to PAR reaching the sediment surface (Fig. 5). Daily integrated system gross production (water

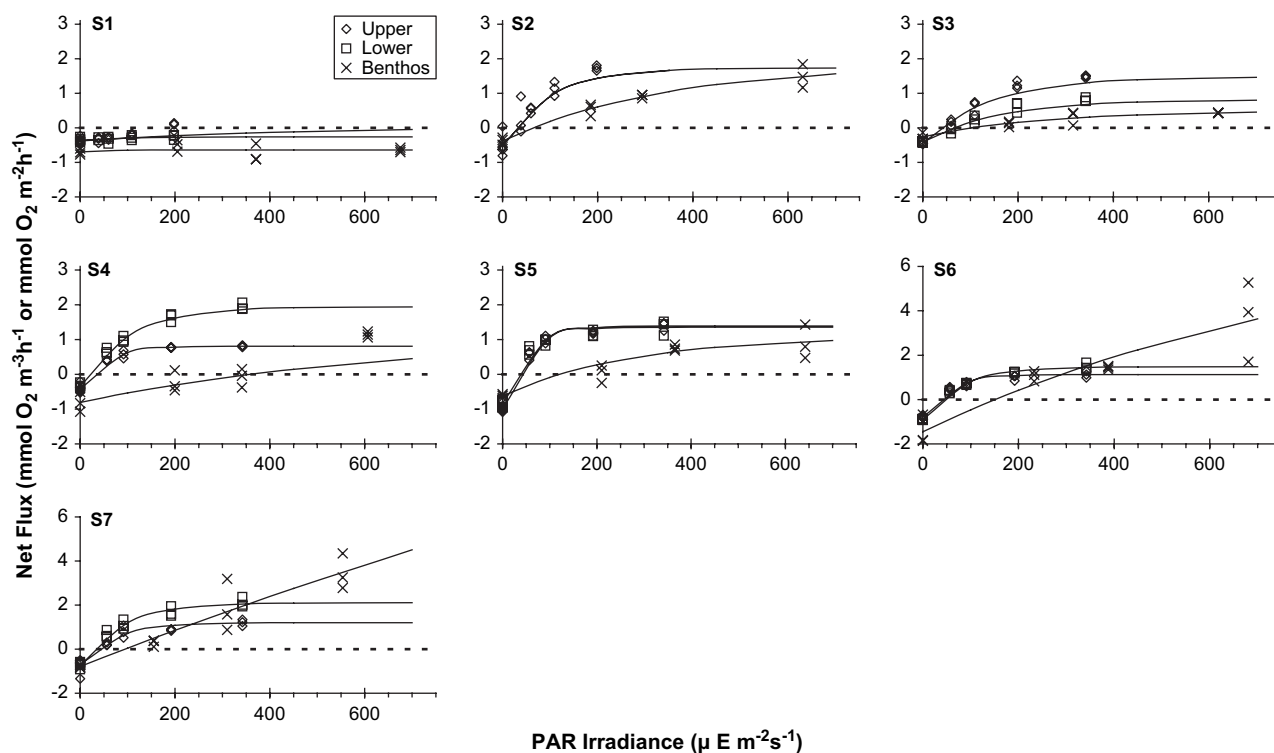


**Fig. 3.** Photosynthesis-irradiance incubation results from the shoal sites, S1 through S7, showing the DO flux response to PAR for the upper water column (diamonds), lower water column (squares), and benthos (X's). The curved lines represent the model fit to observations as described in the text. The horizontal zero lines define the horizon between net production and net respiration. Note the different DO flux units, between water column ( $\text{mmol O}_2 \text{ m}^{-3} \text{ h}^{-1}$ ) and benthos ( $\text{mmol O}_2 \text{ m}^{-2} \text{ h}^{-1}$ ). Also note the expanded vertical scale for station S6 and the lack of lower water column data for station S2.

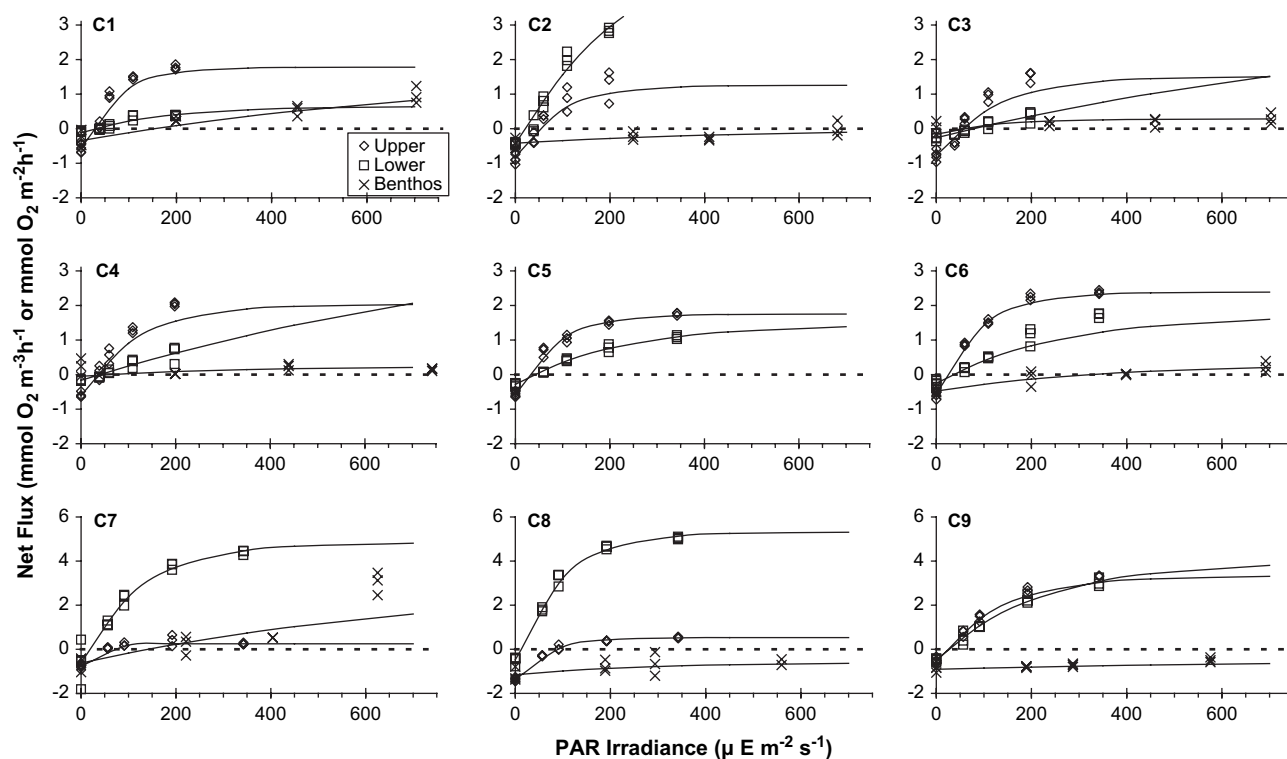


Fig. 4. Photosynthesis-irradiance results from the channel sites, C1 through C9. Other details as in Fig. 3. Note the expanded vertical scale for stations C7, C8 and C9, and the lack of benthic data for station C5.

column + benthos) at channel and shoal sites averaged 69.0 and 37.4  $\text{mmol O}_2 \text{m}^{-2} \text{d}^{-1}$ , respectively (Table 4).

Daily integrated system respiration rates ranged from 19 to 100  $\text{mmol O}_2 \text{m}^{-2} \text{d}^{-1}$  and were about 2-fold higher at channel sites than shoal sites, averaging 68.7 and 34.4  $\text{mmol O}_2 \text{m}^{-2} \text{d}^{-1}$ , respectively (Table 4). Benthic respiration was a larger proportion of total system respiration at shoal stations (50%), compared to channel stations (18%). At stratified channel stations, the upper water column respiration accounted for a larger fraction of integrated plankton respiration than did the lower layer (69% vs. 31%). This difference reflects relative thickness of the layers more than differences in volumetric respiration rates (Figs. 3 and 4).

In this study, system gross production and system respiration were significantly correlated (Fig. 6, Pearson's  $r = 0.61$ ,  $p = 0.01$ ,  $n = 16$ ), and most stations tended to be net autotrophic (above the 1:1 line in Fig. 6). Most of the shoal sites were net autotrophic whereas most of the channel sites were net heterotrophic. One might expect increasing heterotrophy with increasing water depth, but in this study, NEM was not correlated with water depth ( $r = -0.16$ ,  $p = 0.54$ ). Baywide, NEM was nearly balanced, averaging 3.8  $\text{mmol O}_2 \text{m}^{-2} \text{d}^{-1}$  (Table 4).

#### 3.4. Nutrient concentrations and fluxes at the sediment–water interface

Nutrient concentrations and fluxes at the sediment–water interface varied inconsistently among sites and light treatments (Table 5).  $\text{NO}_3^-$  concentrations ranged from 0.2 to 10.8  $\text{mmol m}^{-3}$ , with no obvious spatial patterns.  $\text{NH}_4^+$  concentrations ranged from 0.1 to 11.5  $\text{mmol m}^{-3}$  and DIP concentrations ranged from 0.03 to 1.3  $\text{mmol m}^{-3}$ .  $\text{NO}_3^-$  fluxes ranged between  $-0.7$  and 3.3  $\text{mmol m}^{-2} \text{d}^{-1}$ , with most of the channel sites having a positive flux (Table 5). The effect of light on  $\text{NO}_3^-$  flux was significant ( $t$ -test,  $p < 0.05$ ) at two stations (S3 and S4) with greater uptake of  $\text{NO}_3^-$  in the light than dark (data not shown).  $\text{NH}_4^+$  fluxes ranged between 0 and 3.1  $\text{mmol m}^{-2} \text{d}^{-1}$  with no consistent differences between shoal and channel sites.  $\text{NH}_4^+$  flux was lower ( $t$ -test,  $p < 0.05$ ) in light treatments at 2 sites (S2 and C6; data not shown). DIP fluxes were positive at most of the shoal sites and near zero or negative at channel sites, with no significant light effects. Benthic gross production was positively related to DIP flux, but unrelated to  $\text{NO}_3^-$  or  $\text{NH}_4^+$  flux (Table 6). Compared to silty sites, sandy sites tended to have lower organic content, higher Chl-*a*, higher benthic gross

**Table 3**  
Photosynthetic parameter estimates,  $\alpha^B$  and  $P_m^B$  by water column layer and estuarine depth region  $n$  (shoal/channel). Reported are average, standard error, range, and the number of measurements. Units for  $\alpha^B$  are  $\mu\text{mol O}_2 (\text{mg Chl-}a \text{ h})^{-1}$ . Units for  $P_m^B$  are  $\mu\text{mol O}_2 (\text{mg Chl-}a \text{ h})^{-1}$ .

Region	Layer	$\alpha^B$			$P_m^B$			$n$
		Average	SE	Range	Average	SE	Range	
Shoal	Upper	3.24	0.63	0.53–5.96	285	41	178–441	7
Shoal	Lower	2.99	0.58	1.33–5.49	286	47	127.6–485	7
Shoal	Benthos	0.039	0.01	0.010–0.093	41.8	25.7	2.4–167	6
Channel	Upper	3.22	0.49	1.97–6.61	355	84	175–992	9
Channel	Lower	3.77	0.53	1.73–5.56	1173	211	448–2031	9
Channel	Benthos	0.037	0.01	0.006–0.114	16.5	5.4	2.8–42	8

**Table 4**

Summary of gross production, respiration and net ecosystem metabolism (NEM) for the upper water column (UWC), the lower water column (LWC), and the benthos for each station sampled in Pensacola Bay. The total system values reflect the sum of water column and benthic components. The data are further summarized into shoal, channel, and baywide averages. Baywide averages are weighted to reflect the relative proportion of shoal and channel regions (58% and 42%, respectively). Units are  $\text{mmol O}_2 \text{ m}^{-2} \text{ d}^{-1}$ .

Gross production					Respiration				NEM			
Station	UWC	LWC	Benthic	System	UWC	LWC	Benthic	System	UWC	LWC	Benthic	System
S1	3.5		0.1	3.7	18.8		16.7	35.5	−15.2		−16.5	−31.8
S2	23.6		13.3	36.9	9.9		9.1	19.0	13.6		4.2	17.9
S3	24.3		2.0	26.3	15.5		6.2	21.7	8.9		−4.3	4.6
S4	22.9		8.0	30.9	10.2		19.3	29.5	12.7		−11.3	1.4
S5	32.1		12.1	44.3	24.8		14.9	39.7	7.4		−2.8	4.6
S6	28.8		25.1	53.9	22.3		34.9	57.3	6.5		−9.8	−3.3
S7	31.3		34.3	65.7	18.9		19.1	38.0	12.4		15.3	27.7
C1	71.3	0.9	0.6	72.8	39.7	1.6	8.4	49.7	31.6	−0.7	−7.8	23.1
C2	40.3	6.9	0.1	47.3	38.1	8.7	10.1	56.9	2.2	−1.8	−10.0	−9.6
C3	39.3	3.3	0.0	42.6	31.0	26.3	3.8	61.1	8.2	−22.9	−3.8	−18.5
C4	59.3	0.7	0.0	59.9	41.8	7.1	1.2	50.1	17.5	−6.4	−1.2	9.8
C5	69.5	5.7	–	–	39.3	45.0	–	–	30.3	−39.2	–	–
C6	39.7	30.0	0.1	69.9	14.5	25.7	12.5	52.7	25.3	4.2	−12.3	17.2
C7	30.6	39.1	3.2	72.9	43.9	15.6	11.5	71.0	−13.3	23.5	−8.2	1.9
C8	44.4	29.8	0.3	74.5	68.5	16.3	15.1	100.0	−24.2	13.6	−14.9	−25.5
C9	111.5		0.3	111.8	43.1		27.8	70.9	68.4		−27.6	40.9
Shoal	23.8		13.6	37.4	17.2		17.2	34.4	6.6		−3.6	3.0
Channel	56.2	14.6	0.6	69.0	40.0	18.3	11.3	64.0	16.2	−3.7	−10.7	4.9
Baywide	37.4	14.6	8.1	50.6	26.8	18.3	14.7	46.8	10.6	−3.7	−6.6	3.8

production, higher DIP fluxes, and lower  $\text{NH}_4^+$  fluxes. In Pensacola Bay, availability of organic matter was positively related to  $\text{NH}_4^+$  and  $\text{NO}_3^-$  fluxes and negatively related to DIP flux. Organic matter content was not significantly correlated with benthic respiration, however (Table 6).

#### 4. Discussion

##### 4.1. Role of benthos in total system productivity

The goal of this study was to measure the relative magnitude of benthic and the water column primary production and community respiration in a low-energy, high-light estuarine system. Our results suggest that shoal sediments support substantial production, averaging  $13.6 \pm 4.7 \text{ mmol m}^{-2} \text{ d}^{-1}$  (Table 4), or about 36% of integrated shoal production. At channel sites, benthic production was much lower, <1% of integrated channel production. To normalize rates to the approximate proportion of channel and shoal regions, productivities were weighted by their relative areal

extent assuming a 3 m boundary (42% and 58% of bay area, respectively). This weighting resulted in a baywide average benthic productivity of  $8.1 \text{ mmol O}_2 \text{ C m}^{-2} \text{ d}^{-1}$ , or 16% of total system production (see Table 4). This simple weighting approach likely underestimates shoal productivity somewhat because it does not account for higher production expected in the shallowest regions of the Bay. For example, about 18% (67  $\text{km}^2$ ) of the bay area is shallower than 1 m (Fig. 2), and therefore receives higher irradiance than we simulated in the laboratory. While phytoplankton production typically saturates at  $100\text{--}200 \mu\text{E m}^{-2} \text{ s}^{-1}$ , the sediment microalgae community live in a complex light environment, thus do not exhibit traditional saturation kinetics (MacIntyre et al., 1996). Indeed, our benthic production data showed little evidence of saturation at the highest irradiance ( $\sim 600 \mu\text{E m}^{-2} \text{ s}^{-1}$ , see Figs. 3 and 4). An alternative estimate of benthic production can be calculated by extrapolating the linear trend between irradiance and benthic production (Fig. 5), scaled to the areal distribution of bottom irradiance (Fig. 2). This alternate scaling approach suggests that shoals are about 2-fold more productive than our

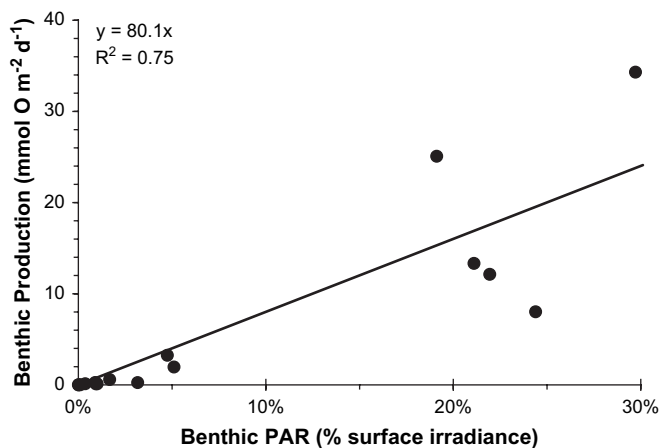


**Fig. 5.** Relationship between benthic gross production and percent of surface irradiance reaching the benthos (% PAR). The data were fit to a linear regression described by the equation Benthic Production = 80.1 X% PAR.

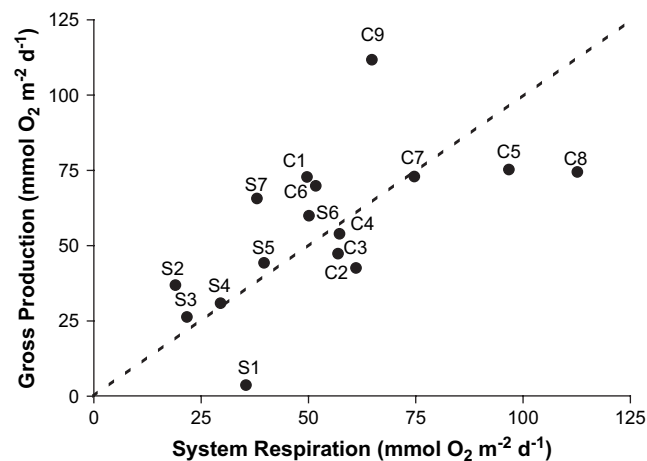


**Fig. 6.** Relationship between total system gross production and system respiration for each station. Stations are labeled to visualize channel vs. shoal patterns. The 1:1 line denotes balanced metabolism.

**Table 5**

Bottom water concentrations and sediment fluxes  $\pm SE$  for dissolved oxygen (i.e., benthic respiration) and inorganic nutrients. DO fluxes represent dark sediment oxygen consumption. Cells with “–” denote missing data. \*Below detection, values represent one half of detection limit. For convenience,  $\text{NO}_3^-$  refers to  $\text{NO}_2^- + \text{NO}_3^-$ , and DIP (dissolved inorganic phosphorus) refers to  $\text{PO}_4^{3-}$ .

Means by Station	DO		$\text{NH}_4^+$		$\text{NO}_3^-$		DIP	
	Concentration ( $\text{mmol O}_2 \text{ m}^{-3}$ )	Flux ( $\text{mmol O}_2 \text{ m}^{-2} \text{ d}^{-1}$ )	Concentration ( $\text{mmol N m}^{-3}$ )	Flux ( $\text{mmol N m}^{-2} \text{ d}^{-1}$ )	Concentration ( $\text{mmol N m}^{-3}$ )	Flux ( $\text{mmol N m}^{-2} \text{ d}^{-1}$ )	Concentration ( $\text{mmol P m}^{-3}$ )	Flux ( $\text{mmol P m}^{-2} \text{ d}^{-1}$ )
S1	150	$16.7 \pm 1.2$	1.8	$2.31 \pm 0.27$	10.8	$0.58 \pm 0.54$	0.03	$-0.07 \pm 0.01$
S2	236	$9.1 \pm 1.5$	1.0	$0.87 \pm 0.15$	5.2	$-0.23 \pm 0.22$	0.30	$0.01 \pm 0.01$
S3	204	$6.2 \pm 1.4$	2.1	$0.03 \pm 0.25$	8.7	$0.63 \pm 0.24$	1.31	$0.05 \pm 0.04$
S4	234	$19.3 \pm 3.9$	4.0	–	0.3	$-0.45 \pm 0.24$	0.20	$0.04 \pm 0.03$
S5	211	$14.9 \pm 0.7$	0.4	$0.31 \pm 0.12$	1.4	$-0.24 \pm 4.45$	0.10*	–
S6	199	$34.9 \pm 9.3$	0.1	$0.19 \pm 0.23$	0.1	$0.06 \pm 0.44$	0.20	$0.24 \pm 0.11$
S7	192	$19.1 \pm 0.9$	0.8	$0.52 \pm 0.35$	0.2	$1.14 \pm 0.39$	0.10*	$0.10 \pm 0.03$
C1	83	$8.4 \pm 3.1$	–	–	3.5	–	0.05	$-0.01 \pm 0.03$
C2	159	$10.1 \pm 2.1$	1.7	$0.73 \pm 0.28$	2.3	$0.40 \pm 0.30$	0.08	$-0.02 \pm 0.01$
C3	42	3.8	–	–	7.0	$-0.12 \pm 0.28$	0.67	$0.02 \pm 0.04$
C4	32	1.2	12.5	–	5.9	$0.96 \pm 0.18$	0.22	$0.00 \pm 0.02$
C6	133	$11.5 \pm 1.6$	8.7	$0.98 \pm 0.31$	2.6	$0.65 \pm 0.30$	0.53	$0.05 \pm 0.03$
C7	143	$15.1 \pm 4.9$	0.1	$3.07 \pm 1.16$	0.2	$2.19 \pm 1.11$	0.20	$-0.07 \pm 0.07$
C8	150	$27.8 \pm 4.5$	0.05*	$2.12 \pm 1.50$	10.5	$3.28 \pm 1.05$	0.10*	$-0.12 \pm 0.03$
C9	179	$21.7 \pm 1.8$	3.0	$1.15 \pm 0.40$	0.2	$-0.74 \pm 0.44$	0.20	$-0.05 \pm 0.03$
<i>Means by location</i>								
Shoal	204	$17.2 \pm 9.3$	1.45	$0.70 \pm 0.84$	3.81	$0.21 \pm 0.58$	0.32	$0.06 \pm 0.11$
Channel	115	$12.5 \pm 8.9$	4.34	$1.61 \pm 0.97$	4.02	$0.95 \pm 1.38$	0.25	$-0.03 \pm 0.05$
All Stations	156	$4.7 \pm 9.1$	2.79	$1.11 \pm 0.98$	3.93	$0.58 \pm 1.08$	0.29	$0.01 \pm 0.09$

measurements suggest ( $27.1$  vs.  $13.6 \text{ mmol O}_2 \text{ m}^{-2} \text{ d}^{-1}$ ). This extrapolation suggests average baywide benthic productivity (channel + shoal) is also about 2-fold higher than our direct measurements ( $16.5$  vs.  $8.1 \text{ mmol O}_2 \text{ m}^{-2} \text{ d}^{-1}$ ) or about 32% of total system gross production.

Cahoon (1999) compiled benthic productivity data from intertidal and subtidal environments, ranging from tropical to polar latitudes. This synthesis (85 studies) observed that high benthic productivity is typical of shallow reaches of systems, particularly in temperate ( $30$ – $60^\circ$ ) and tropical ( $0$ – $30^\circ$ ) latitudes, with averages ranging from  $87$  to  $576 \text{ g C m}^{-2} \text{ y}^{-1}$ , respectively. The comparable shoal productivity for Pensacola Bay ( $27.1 \text{ mmol O}_2 \text{ m}^{-2} \text{ d}^{-1}$ ), when converted to annual carbon equivalents ( $\text{PQ} = 1$ ) is  $119 \text{ g C m}^{-2} \text{ y}^{-1}$ , on the low end the reported range. Benthic Chl-*a* in the Pensacola Bay shoals averaged  $206 \text{ mg m}^{-2}$ , near the center of the reported range ( $128$  and  $347 \text{ mg Chl-}a \text{ m}^{-2}$ ) for temperate and tropical systems, respectively (Cahoon, 1999).

#### 4.2. Photosynthesis–irradiance relationships

Algal photosynthetic parameters are sensitive to environmental and physiological factors, including incident irradiance patterns, species composition, geographic location, and ambient nutrient concentrations (e.g., Cote and Platt, 1983; Lohrenz et al., 1994; Falkowski and Raven, 1997; MacIntyre et al., 2002). Our water

column parameter estimates,  $\alpha^B$  and  $P_m^B$ , were similar to those reported in these studies, both in terms of magnitude and variability. However, benthic  $P$ – $I$  parameter estimates are more difficult to compare among studies due to different normalization approaches and incubation methods. Light and Beardall (2001) recently reviewed benthic  $P$ – $I$  parameters, finding a wide range in both  $\alpha^B$  and  $P_m^B$  among the studies examined. They reported benthic  $\alpha^B$  ranging from  $0.11$  to  $21.9 \text{ } \mu\text{mol O}_2 (\text{mg Chl-}a \text{ h})^{-1} (\mu\text{E m}^{-2} \text{ s}^{-1})$  and benthic  $P_m^B$  ranging from  $3.1$  to  $2000 \text{ } \mu\text{mol O}_2 (\text{mg Chl-}a \text{ h})^{-1}$  when converted to equivalent molar units. In comparison, our benthic  $\alpha^B$  averaged  $0.038 \text{ } \mu\text{mol O}_2 (\text{mg Chl-}a \text{ h})^{-1} (\mu\text{E m}^{-2} \text{ s}^{-1})$ , roughly one third of the minimum reported in the review. Similarly, our average benthic  $P_m^B$  (for shoal stations only) was  $42 \text{ } \mu\text{mol O}_2 (\text{mg Chl-}a \text{ h})^{-1}$ , at the low end reported in Light and Beardall (2001). While some of the variability among studies reflect true differences in microphytobenthic photosynthetic properties, artifacts arise from experimental and normalization methods. A major inconsistency among investigators is the thickness of sediment samples used for chlorophyll normalization. In this study, we sampled the top 10 mm of sediment for Chl-*a*, which is thicker than many studies (range 2–10 mm, Light and Beardall, 2001). Had we sampled only the top 2 mm of sediment to determine Chl-*a*, our normalized parameter estimates could have been up to 5-fold higher, and closer to the center of the literature-reported range of values.

**Table 6**

Pearson correlation coefficients for dissolved oxygen at the sediment–water interface, sediment characteristics, sediment oxygen production, sediment respiration, and inorganic nutrient fluxes. Values in bold are significant at  $p < 0.05$ ; values in bold with asterisk (\*) are significant at  $p < 0.01$ . The number of observations ranged from 10 to 16.

	Bottom DO	Benthic Chl- <i>a</i>	% Sand	% LOI	Benthic GPP	Benthic Resp	Benthic NPP	$\text{NH}_4^+$ Flux	$\text{NO}_3^-$ Flux
Benthic Chl- <i>a</i>	0.47								
% Sand	<b>0.70</b>	<b>0.63</b>							
% LOI	<b>–0.57</b>	<b>–0.68*</b>	<b>–0.96*</b>						
Benthic GPP	0.49	0.33	<b>0.62</b>	–0.50					
Benthic Resp	<b>0.50</b>	–0.16	0.05	–0.01	0.46				
Benthic NPP	0.06	0.48	0.58	–0.50	<b>0.63</b>	–0.40			
$\text{NH}_4^+$ Flux	<b>–0.66*</b>	–0.51	<b>–0.83*</b>	<b>0.90*</b>	–0.45	0.09	<b>–0.52</b>		
$\text{NO}_3^-$ Flux	–0.26	–0.31	–0.37	<b>0.54</b>	–0.11	0.16	–0.25	<b>0.60</b>	
DIP Flux	0.27	0.51	<b>0.65</b>	<b>–0.65</b>	<b>0.71*</b>	0.26	0.50	<b>–0.75</b>	–0.42



#### 4.3. Benthic respiration

In a literature synthesis, [Hopkinson and Smith \(2005\)](#) summarized system respiration rates from 48 estuarine sites reporting a range from 3 to 115 mmol C m<sup>-2</sup> d<sup>-1</sup> (estimated from their Fig. 8.1). Our average of 15.2 mmol C m<sup>-2</sup> d<sup>-1</sup> (assuming O<sub>2</sub>:C = 1) is at the lower end of this large group of estuaries. The relatively low benthic respiration rates seem reasonable given the moderate to low overall productivity of Pensacola Bay ([Murrell et al., 2007](#)), and the proportionally large area of sandy, low organic sediments. While benthic respiration did not vary strongly with depth, channel respiration rates (12.5 ± 2.8 mmol O<sub>2</sub> m<sup>-2</sup> d<sup>-1</sup>) were lower than shoal respiration rates (17.2 ± 3.5 mmol O<sub>2</sub> m<sup>-2</sup> d<sup>-1</sup>). This result was surprising given that channel sites had higher organic content than shoal sites (9.4% vs. 2.2%), and therefore should support higher respiration rates. One explanation is that channel sites were more often hypoxic, which would limit sediment respiratory oxygen consumption. Indeed, there was a significant correlation between initial bottom water DO concentration and benthic respiration ( $r = 0.50$ ,  $p < 0.05$ ,  $n = 16$ ).

Another possible explanation for the higher shoal respiration rates is that the sandy sediments characteristic of the shoals are more permeable, thus are subject to larger advective flow through the pore waters. This increased flow facilitates solute exchange, thus supporting more rapid recycling of organic matter ([Huettel and Rusch, 2000](#)). Elevated respiration rates attributable to advective flow through permeable sediments have been observed in high energy intertidal zones ([De Beer et al., 2005](#)) and on continental shelves ([Rusch et al., 2006](#)). Our rates from sandy sites probably underestimate true respiration because we enclosed sediments in core tubes, thus isolating the sediments from pore water advection ([Janssen et al., 2005](#); [Cook et al., 2007](#)). While it is difficult to estimate the magnitude of this bias, advective exchanges in Pensacola Bay are likely less important than observed in physically dominated, eutrophic systems, given the low tidal energy and low organic content of the sandy shoal sediments. Another factor that often leads to lower measured fluxes in cores compared to in situ chambers is that cores tend to under-represent or disrupt the bioturbation effects of macrofauna ([Rabouille et al., 2003](#); [Hammond et al., 2004](#)). This magnitude of this effect is also likely small in Pensacola Bay because benthic macrofauna appear to be dominated more by surface dwelling spionids and capitellids (EPA unpublished data).

#### 4.4. Sediment fluxes and nutrient recycling

Nutrient fluxes in this study were similar to previous measurements made in Pensacola Bay ([DiDonato et al., 2006](#); [Smith and Caffrey, in press](#)). NH<sub>4</sub><sup>+</sup> fluxes tended to be higher in the channel than shoals and were also larger than NO<sub>3</sub><sup>-</sup> fluxes. DIP fluxes were near zero at shoal sites and were negative in the channel. Thus, the hypoxic conditions in Pensacola Bay appear insufficient to induce DIP efflux, as observed under anoxic conditions in Chesapeake Bay and the Baltic Sea ([Koop et al., 1990](#); [Cowan and Boynton, 1996](#)). In this respect, Pensacola Bay appears similar to Mobile Bay, which did not experience enhanced DIP efflux under hypoxic conditions ([Cowan et al., 1996](#)). Like many Gulf of Mexico estuaries, Pensacola Bay rarely if ever goes completely anoxic ([Hagy and Murrell, 2007](#)), therefore may not experience the benthic nutrient recycling feedback effects that accentuate eutrophication in anoxic systems.

Overall, the effect of light on benthic nutrient fluxes in Pensacola Bay was small compared to other systems. In the Kattgat and lower Chesapeake Bay, benthic nutrient fluxes in the light were significantly lower than those measured in the dark ([Sundbäck et al., 1991](#); [Reay et al., 1995](#); [Sundbäck et al., 2000](#)), consistent with

light-mediated uptake of nutrients by the microphytobenthos. However, in the Limfjorden system, there was no light effect on benthic nutrient fluxes ([Dalsgaard, 2003](#)). This pattern, along with generally low pore water nutrient concentrations ([Smith and Caffrey, in press](#); [Caffrey et al., 2007](#)) suggest that shallow sediments were not a significant reservoir of nutrients and that microphytobenthic nutrient requirements were met by active recycling and exchange with the overlying water column. This interpretation is consistent with a previous study that observed active water column nutrient cycling based on phytoplankton productivity, nutrient distributions, and flushing characteristics ([Murrell et al., 2007](#)).

The influence of microphytobenthos on nutrient fluxes should be greater in shallow depths ([Rizzo and Christian, 1992](#); [Sundbäck et al., 2004](#)), primarily due to higher microphytobenthic biomass and productivity in the shoals. In contrast with [Sundbäck et al. \(2004\)](#), we did not observe the expected negative relationships between benthic gross production and nutrient fluxes ([Table 6](#)). Nevertheless, active recycling of nutrients in euphotic sediments can be critical for maintaining microphytobenthic production ([Sundbäck et al., 2000](#)). For example, [Sundbäck et al. \(2006\)](#) found that microphytobenthos were responsible for 40–100% of uptake of remineralized N, while denitrification represented only about 5%. As a means of estimating the magnitude of sediment nutrient recycling in Pensacola Bay, we converted benthic respiration rate data into predicted DIN (=NO<sub>3</sub><sup>-</sup> + NH<sub>4</sub><sup>+</sup>) and DIP mineralization rates (assuming Redfield stoichiometry and RQ = 1). The comparison of predicted and observed DIN and DIP fluxes is plotted in [Fig. 7](#). For DIN, points falling above the 1:1 line imply that either nitrogen fixation is a source of DIN or that benthic respiration underestimates remineralization. Benthic respiration can underestimate carbon mineralization when there is accumulation of reduced end-products of organic matter mineralization such as S<sup>2-</sup>, Fe<sup>2+</sup>, or methane. Points falling below the 1:1 line imply a net sink of nutrients to the system. For DIN, most sites were very close to the 1:1 line suggesting that the DIN remineralized could be accounted for by the benthic fluxes with minimal denitrification. The shoal sites that fell furthest below the 1:1 line had high gross production, suggesting significant dark uptake by microphytobenthos. As for DIP, most sites fell below the 1:1 line implying the system is a net sink for phosphorus, by two principle mechanisms: algal uptake or P adsorption onto minerals (e.g., ferric oxyhydroxides). At the channel sites, mineral adsorption of DIP was likely more important because these sites had negligible photosynthesis. In contrast, the shoal sites should have higher DIP uptake by microphytobenthos to support the observed primary production rates. Mineral adsorption of DIP is expected to be small due to the low iron content of the sandy sediments relative to the silty channel sites (unpublished data). Contrary to expectations, we observed a positive relationship between DIP flux and gross production ( $r = 0.71$ ,  $p < 0.01$ ,  $n = 14$ ), a result that belies a simple explanation. Thus, it appears that phosphorus cycling in Pensacola Bay is complex, requiring more focused study to understand pathways of DIP uptake and remineralization.

#### 4.5. Below pycnocline net production and hypoxia

Many of the well-studied hypoxic or anoxic marine systems, such as Chesapeake Bay, the Baltic Sea, or the Louisiana Continental Shelf (reviewed by [Diaz and Rosenberg, 2001](#)) are relatively turbid and deep, such that bottom waters are too dark to support primary production. Pensacola Bay is an example of a shallow, stratified estuary with relatively low turbidity, therefore significant light

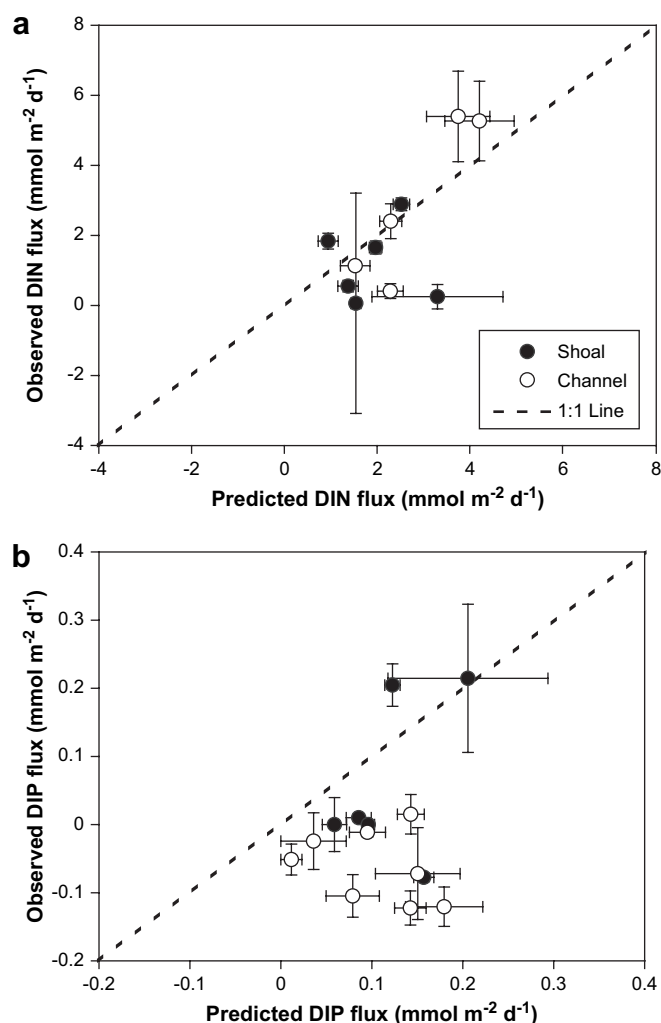


**Fig. 7.** Relationship between observed and predicted DIN (a) and DIP (b) fluxes at the sediment-water interface. Predicted fluxes were calculated from benthic respiration measurements by applying Redfield scaling (106 O: 16 N: 1 P). The error bars represent the standard errors of the measurements. The symbols indicate shoal filled circles and channel (open circles) sites. The line represents the 1:1 relationship.

penetrates below the pycnocline and to the sediment surface. This light is capable of supporting primary production that acts to offset respiratory oxygen demand, and potentially reduces the occurrence of hypoxia. Our results (Table 7) show that below-pycnocline gross production was significant ( $14.6 \pm 5.5 \text{ mmol O}_2 \text{ m}^{-2} \text{ d}^{-1}$ ), nearly completely offsetting community respiration ( $18.3 \pm 4.9 \text{ mmol O}_2 \text{ m}^{-2} \text{ d}^{-1}$ ). This finding is consistent with a previous box-model study in Pensacola Bay that showed net DO flux below the pycnocline was nearly balanced (Hagy and Murrell, 2007). This prior study also calculated vertical oxygen exchange rates that were extremely sluggish suggesting that hypoxia can develop with only a slight imbalance between production and respiration. Thus, Pensacola Bay is naturally susceptible to hypoxia and the extent of hypoxia is sensitive to changes in light availability below the pycnocline. While the rivers draining into Pensacola Bay do not currently carry large sediment loads (e.g., Escambia River suspended solids average  $9.3 \text{ mg l}^{-1}$ , EPA unpublished data), disturbance of the landscape could increase erosion, sediment transport, and turbidity. This provides a mechanism in addition to anthropogenic nutrient enrichment by which landscape disturbance could contribute to increased hypoxia.

**Table 7**

Below pycnocline gross production (GPP), community respiration (CR), and net production (NPP) at stratified sites. Units are  $\text{mmol O}_2 \text{ m}^{-2} \text{ d}^{-1}$ . Also included is the percent of surface irradiance (% PAR) reaching the pycnocline. Averages ( $\pm$ SE) are included.

Station	GPP	CR	NPP	% PAR
C1	0.9	1.6	-0.7	4%
C2	6.9	8.7	-1.8	5%
C3	3.3	26.3	-22.9	10%
C4	0.7	7.1	-6.4	2%
C5	5.7	45.0	-39.2	5%
C6	30.0	25.7	4.2	33%
C7	39.1	15.6	23.5	14%
C8	29.8	16.3	13.6	7%
Average	$14.6 \pm 5.5$	$18.3 \pm 4.9$	$-3.7 \pm 7.0$	$9.8\% \pm 3.5\%$

#### 4.6. Net ecosystem metabolism

Net ecosystem metabolism among the 16 stations in this study showed the majority of sites were net autotrophic (see Fig. 6), but taken together, were not statistically different from zero, implying the system is in near metabolic balance. Previous studies have observed that within an estuarine system, NEM tended to become more heterotrophic with increasing water depth (Kemp et al., 1997; Caffrey et al., 1998). This depth trend is consistent with the observation that estuarine productivity is typically light limited due to high turbidity, whereas water column integrated respiration continues to increase with increasing water depth. In contrast, Pensacola Bay has low turbidity and high light penetration (see Fig. 2), thus primary production occurs through much of the water column and benthos. The high light environment and generally low benthic respiration rates likely explains why NEM in Pensacola Bay was unrelated to water depth (Pearson's  $r = -0.16$ ,  $p = 0.54$ ).

Because this study was conducted during summer, the observed production and respiration rates do not adequately represent the other seasons. Prior studies of Pensacola Bay have observed relatively muted inter-seasonal variability ( $\sim 2$ -fold) in primary production (Murrell et al., 2007) and higher variability ( $\sim 10$ -fold) in heterotrophic processes such as bacterioplankton production (Murrell, 2003). This implies an apparent decoupling between autotrophic and heterotrophic processes spring being the most autotrophic when production is highest and respiration is relatively low. In contrast, summer would tend to be most heterotrophic when primary production becomes nutrient-limited and respiration rates peak with high temperatures. Indeed, this sort of inter-seasonal pattern in NEM was observed by Caffrey (2004) in a multi-system comparison.

Based on the above, it is likely that annual NEM rates for Pensacola Bay are higher than the summer rates reported here. Nevertheless, when compared to annual estimates from other estuarine and coastal systems, Pensacola Bay has relatively low summer productivity and high NEM (Fig. 8). In this regard, it is similar to Moreton Bay, Australia (Eyre and McKee, 2002), Narragansett Bay, Rhode Island, USA (Nixon et al., 1995; LOICZ, 2003), and several systems reported in Smith and Hollibaugh (1993). Compared to Pensacola Bay, Chesapeake Bay and Waquoit Bay have similar NEM but much higher gross primary production, likely due to high anthropogenic inorganic nutrient inputs (D'Avanzo and Kremer, 1994; Kemp et al., 1997). These high NEM systems contrast with many estuarine systems reported in Caffrey (2004) that have significant allochthonous organic carbon inputs and hence are strongly heterotrophic. Thus, low inputs of organic matter and high light levels appear to support high NEM in Pensacola Bay despite relatively low nutrient inputs.

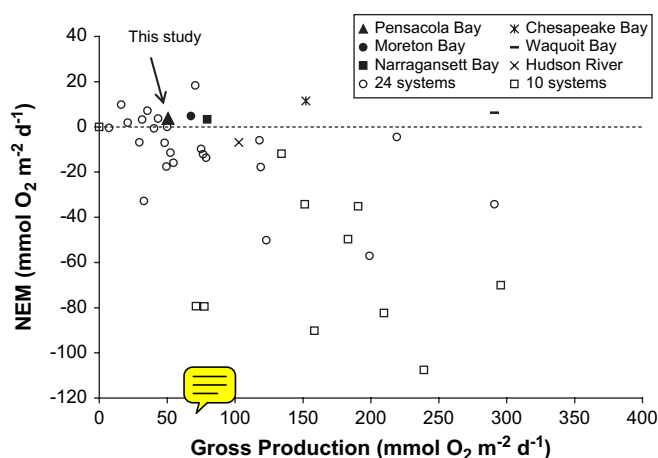


**Fig. 8.** Relationship between net ecosystem metabolism (NEM) and gross production among various estuarine and coastal systems reported in the literature. When necessary, literature values were converted to equivalent daily molar oxygen units assuming  $RQ=PQ=1$ . Included are 24 estuarine and coastal systems reported in Smith and Hollibaugh (1993), 10 estuarine systems reported in Caffrey (2004), Moreton Bay (Eyre and McKee, 2002), Waquoit Bay (D'Avanzo and Kremer, 1994), Narragansett Bay (Nixon et al., 1995 and LOICZ, 2003), Hudson River (Howarth et al., 1996) and Chesapeake Bay (Kemp et al., 1997). Pensacola Bay data are baywide averages as reported in Table 4.

## 5. Conclusions

High light levels reaching the bottom of Pensacola Bay support benthic production that accounts for as much as 32% of the baywide gross production. High light below the pycnocline supports production that helps reduce, but does not eliminate, hypoxia in this strongly stratified microtidal estuary. Nutrient concentrations at the sediment–water interface were moderate, and nutrient recycling, particularly DIP, appears critical to support the micro-phytobenthic community. Compared to other estuaries, Pensacola Bay has relatively low productivity and high net ecosystem metabolism.

## Acknowledgments

This study was made possible by the excellent field and lab support provided by R. Quarles, L. Smith, V. Engle, R. Stanley, H. Reed, K. Smith, and S. Duffy. Helpful comments from R. Greene, J. Lehrter, E. Smith, and several anonymous reviewers have improved the manuscript. This study was funded by the US EPA, National Health and Environmental Effects Research Laboratory. J. Caffrey received support from a National Science Foundation grant (OCE-0352221). The contents are solely the views of the authors and use of trade names or commercial products does not constitute endorsement. Contribution # 1339 from the Gulf Ecology Division.

## References

- An, S., Joye, S.B., 2001. Enhancement of coupled nitrification–denitrification by benthic photosynthesis in shallow estuarine sediments. *Limnology and Oceanography* 46, 62–74.
- APHA, 1989. Standard Methods for the Examination of Water and Wastewater. APHA (American Public Health Association), Washington, DC.
- Bianchi, T.S., Pennock, J.R., Twilley, R.R. (Eds.), 1999. Biogeochemistry of Gulf of Mexico Estuaries. John Wiley & Sons, New York, 428 pp.
- Bricker, S., Longstaff, B., Dennison, W., Jones, A., Boicourt, K., Wicks, C., Woerner, J., 2007. Effects of Nutrient Enrichment in the Nation's Estuaries: A Decade of Change. NOAA, Coastal Ocean Program, Decision Analysis Series No 26. National Centers for Coastal Ocean Science, Silver Spring, MD, 322 pp.
- Caffrey, J.M., 2004. Factors controlling net ecosystem metabolism in U.S. estuaries. *Estuaries* 27, 90–101.

- Caffrey, J.M., Bano, N., Kalanetra, K., Hollibaugh, J.T., 2007. Ammonia oxidation and ammonia-oxidizing bacteria and Archaea from estuaries with differing histories of hypoxia. *International Society for Microbial Ecology* 1, 660–662.
- Caffrey, J.M., Cloern, J.E., Grenz, C., 1998. Changes in production and respiration during a spring phytoplankton bloom in San Francisco Bay, California, USA: implications for net ecosystem metabolism. *Marine Ecology Progress Series* 172, 1–12.
- Cahoon, L.B., 1999. The role of benthic microalgae in neritic ecosystems. *Oceanography and Marine Biology Annual Review* 37, 47–86.
- Cook, P.L.M., Wenzhöfer, F., Glud, R.N., Janssen, F., Huettel, M., 2007. Benthic solute exchange and carbon mineralization in two shallow subtidal sandy sediments: effect of advective pore-water exchange. *Limnology and Oceanography* 52, 1943–1963.
- Cote, B., Platt, T., 1983. Day-to-day variations in the spring–summer photosynthetic parameters of coastal marine phytoplankton. *Limnology and Oceanography* 28, 320–344.
- Cowan, J.L.W., Pennock, J.R., Boynton, W.R., 1996. Seasonal and interannual patterns of sediment–water nutrient and oxygen fluxes in Mobile Bay, Alabama (USA): regulating factors and ecological significance. *Marine Ecology Progress Series* 141, 229–245.
- Cowan, J.L., Boynton, W.R., 1996. Sediment–water oxygen and nutrient exchanges along the longitudinal axis of Chesapeake Bay: seasonal patterns, controlling factors and ecological significance. *Estuaries* 19, 561–580.
- Dalsgaard, T., 2003. Benthic primary production and nutrient cycling in sediments with benthic microalgae and transient accumulation of macroalgae. *Limnology and Oceanography* 48, 2138–2150.
- D'Avanzo, C., Kremer, J.N., 1994. Diel oxygen dynamics and anoxic events in an eutrophic estuary of Waquoit Bay, Massachusetts. *Estuaries* 17, 131–139.
- De Beer, D., Wenzhöfer, F., Ferdelman, T.G., Boehme, S.E., Huettel, M., van Beusekom, J.E.E., Bottcher, M.E., Musat, N., Dubilier, N., 2005. Transport and mineralization rates in North Sea sandy intertidal sediments, Sylt–Romo Basin, Wadden Sea. *Limnology and Oceanography* 50, 113–127.
- Diaz, R.J., Rosenberg, R., 2001. Overview of anthropogenically-induced hypoxic events on marine benthic fauna. In: Rabalais, N.N., Turner, R.E. (Eds.), *Coastal Hypoxia: Consequences for Living Resources and Ecosystems*. American Geophysical Union, Washington, DC, pp. 129–146.
- DiDonato, G.T., Lores, E.M., Murrell, M.C., Smith, L., Caffrey, J.M., 2006. Benthic nutrient flux in a small estuary in northwestern Florida. *Gulf and Caribbean Research* 18, 15–25.
- Eyre, B.D., McKee, L.J., 2002. Carbon, nitrogen, and phosphorus budgets for a shallow subtropical coastal embayment (Moreton Bay, Australia). *Limnology and Oceanography* 47, 1043–1055.
- Falkowski, P.G., Raven, J.A., 1997. *Aquatic Photosynthesis*. Blackwell Science, Malden, Mass, 484 pp.
- Folk, R.L., 1974. *Petrology of Sedimentary Rocks*. Hemphill Publishing Co., Austin, Texas, 182 pp.
- Hagy III, J.D., Murrell, M.C., 2007. Susceptibility of a Gulf of Mexico estuary to hypoxia: an analysis using box models. *Estuarine, Coastal and Shelf Science* 74, 239–253.
- Hagy III, J.D., Lehrter, J.C., Murrell, M.C., 2006. Effects of hurricane Ivan on water quality in Pensacola Bay, FL USA. *Estuaries and Coasts* 29, 919–925.
- Hammond, D.E., Cummins, K.M., Mcmanus, J., Berelson, W.M., Smith, G., Spagnoli, F., 2004. Methods for measuring benthic nutrient flux on the California Margin: comparing shipboard core incubations to in situ lander results. *Limnology and Oceanography Methods* 2, 146–159.
- Handley, L., Altsman, D., DeMay, R., 2007. Seagrass Status and Trends in the Northern Gulf of Mexico: 1940–2002. U.S. Geological Survey Investigations Report 2006–5287 and U.S. Environmental Protection Agency 855-R-04-003, Washington, DC, 267 pp.
- Hopkinson Jr., C.S., Smith, E.M., 2005. Estuarine respiration: an overview of benthic, pelagic, and whole system respiration. In: Del Giorgio, P.A., Williams, P.J.le B. (Eds.), *Respiration in Aquatic Systems*. Oxford University Press, New York, pp. 122–146.
- Howarth, R.W., Schneider, R., Swaney, D., 1996. Metabolism and organic carbon fluxes in the tidal freshwater Hudson River. *Estuaries* 19, 848–865.
- Huettel, M., Rusch, A., 2000. Transport and degradation of phytoplankton in permeable sediment. *Limnology and Oceanography* 45, 534–549.
- Janssen, F., Huettel, M., Witte, U., 2005. Pore-water advection and solute fluxes in permeable marine sediments (II): benthic respiration at three sandy sites with different permeabilities. *Limnology and Oceanography* 50, 779–792.
- Kemp, W.M., Smith, E.M., Marvin-DiPasquale, M., Boynton, W.R., 1997. Organic carbon balance and net ecosystem metabolism in Chesapeake Bay. *Marine Ecology Progress Series* 150, 229–248.
- Koop, K., Boynton, W.R., Wulff, F., Carman, R., 1990. Sediment–water oxygen and nutrient exchanges along a depth gradient in the Baltic Sea. *Marine Ecology Progress Series* 63, 65–77.
- Light, B.R., Beardall, J., 2001. Photosynthetic characteristics of sub-tidal benthic microalgal populations from a temperate, shallow water marine ecosystem. *Aquatic Botany* 70, 9–27.
- Lohrenz, S.E., Fahnenstiel, G.L., Redalje, D.G., 1994. Spatial and temporal variations of photosynthetic parameters in relation to environmental conditions in coastal waters of the northern Gulf of Mexico. *Estuaries* 17, 779–795.
- LOICZ, 2003. Land–Ocean interactions in the coastal zone, biogeochemical modeling node. Available from: <http://data.ecology.su.se/MNODE/>.

- MacIntyre, H.L., Geider, R.J., Miller, D.C., 1996. Microphytobenthos: the ecological role of the “secret garden” of unvegetated, shallow-water marine habitats. I. Distribution, abundance and primary production. *Estuaries* 19, 186–201.
- MacIntyre, H.L., Kana, T.M., Geider, R.J., 2002. Photoacclimation of photosynthesis irradiance response curves and photosynthetic pigments in microalgae and cyanobacteria. *Journal of Phycology* 38, 17–38.
- Miller-Way, T., Boland, G.S., Rowe, G.T., Twilley, R.R., 1994. Sediment oxygen consumption and benthic nutrient fluxes on the Louisiana continental shelf: a methodological comparison. *Estuaries* 17, 809–815.
- Murrell, M.C., 2003. Bacterioplankton dynamics in a subtropical estuary, evidence for substrate limitation. *Aquatic Microbial Ecology* 32, 239–250.
- Murrell, M.C., Hagy III, J.D., Lores, E.M., Greene, R., 2007. Phytoplankton production and nutrient distributions in a sub-tropical estuary: importance of freshwater flow. *Estuaries and Coasts* 30, 390–402.
- NRC (National Research Council), 2000. *Clean Coastal Waters: Understanding the Effects of Nutrient Pollution*. National Academy Press, Washington, DC, 405 pp.
- Nixon, S.W., Granger, S.L., Nowicki, B.L., 1995. An assessment of the annual mass balance of carbon, nitrogen and phosphorus in Narragansett Bay. *Biogeochemistry* 31, 15–61.
- Park, K., Kim, C.-K., Schroeder, W.W., 2007. Temporal variability in summertime bottom hypoxia in shallow areas of Mobile Bay, Alabama. *Estuaries and Coasts* 30, 54–65.
- Platt, T., Sathyendranath, S., Ravindran, P., 1990. Primary production by phytoplankton: analytic solutions for the daily rates per unit area of water surface. *Proceedings of the Royal Society London B*, 101–111.
- Rabouille, C., Denis, L., Dedieu, K., Stora, G., Lansard, B., Grenz, C., 2003. Oxygen demand in coastal marine sediments: comparing in situ microelectrodes and laboratory core incubations. *Journal of Experimental Marine Biology and Ecology* 285–286, 49–69.
- Reay, W.G., Gallagher, D.L., Simmons Jr., G.M., 1995. Sediment-water column oxygen and nutrient fluxes in nearshore environments of the lower Delmarva Peninsula. *Marine Ecology Progress Series* 118, 215–227.
- Rizzo, W.M., Christian, R.R., 1992. Significance of subtidal sediments to heterotrophically mediated oxygen and nutrient dynamics in a temperate estuary. *Estuaries* 19, 475–487.
- Rusch, A., Huettel, M., Wild, C., Reimers, C.E., 2006. Benthic oxygen consumption and organic matter turnover in organic-poor permeable shelf sands. *Aquatic Geochemistry* 12, 1–19.
- Schroeder, W.W., Wiseman Jr., W.J., 1999. Geology and hydrodynamics of Gulf of Mexico Estuaries. In: Bianchi, T.S., Pennock, J.R., Twilley, R.R. (Eds.), *Biogeochemistry of Gulf of Mexico Estuaries*. John Wiley and Sons, Inc, New York, pp. 3–28.
- Schreiber, R.A., Pennock, J.R., 1995. The relative contribution of benthic and microalgae to total microalgal production in a shallow sub-tidal estuarine environment. *Ophelia* 42, 335–352.
- Smith, K.A., Caffrey, J.M. The effects of human activities and extreme meteorological events on sediment nitrogen dynamics in an urban estuary, Escambia Bay, Florida, USA. *Hydrobiologia*, in press.
- Smith, S.V., Hollibaugh, J.T., 1993. Coastal metabolism and the oceanic organic carbon balance. *Reviews of Geophysics* 31, 75–89.
- Stutes, A.L., Cebrian, J., Corcoran, A.A., 2006. Effects of nutrient enrichment and shading on sediment primary production and metabolism in eutrophic estuaries. *Marine Ecology Progress Series* 312, 29–43.
- Sundbäck, K., Enoksson, V., Graneli, W., Pettersson, K., 1991. Influence of sublittoral microphytobenthos on the oxygen and nutrient flux between sediment and water: a laboratory continuous-flow study. *Marine Ecology Progress Series* 74, 263–279.
- Sundbäck, K., Linares, F., Larson, F., Wulff, A., 2004. Benthic nitrogen fluxes along a deep gradient in a microtidal fjord: the role of denitrification and microphytobenthos. *Limnology and Oceanography* 49, 1095–1107.
- Sundbäck, K., Miles, A., Goransson, E., 2000. Nitrogen fluxes, denitrification and the role of microphytobenthos in microtidal shallow-water sediments: an annual study. *Marine Ecology Progress Series* 200, 59–76.
- Sundbäck, K., Miles, A., Linares, F., 2006. Nitrogen dynamics in nontidal littoral sediments: role of microphytobenthos and denitrification. *Estuaries and Coasts* 29, 1196–1211.
- Turner, R.E., 2001. Of manatees, mangroves, and the Mississippi River: is there an estuarine signature for the Gulf of Mexico? *Estuaries* 24, 139–150.
- Twilley, R.R., Cowan, J., Miller-Way, T., Montagna, P.A., Mortazavi, B., 1999. Benthic nutrient fluxes in selected estuaries in the Gulf of Mexico. In: Bianchi, T.S., Pennock, J.R., Twilley, R.R. (Eds.), *Biogeochemistry of Gulf of Mexico Estuaries*. John Wiley and Sons, Inc, New York, pp. 163–209.
- US EPA (US Environmental Protection Agency), 2001. *National Coastal Condition Report*. Office of Research and Development/Office of Water, Washington, DC, 204 pp.
- Welschmeyer, N.A., 1994. Fluorometric analysis of chlorophyll-a in the presence of chlorophyll-b and phaeopigments. *Limnology and Oceanography* 39, 1985–1992.